sd-shell observables for the USDA and USDB Hamiltonians

W. A. Richter,[1] S. Mkhize,[1] and B. Alex Brown[2]
[1]*Department of Physics, University of the Western Cape, Private Bag X17, Bellville 7535, South Africa*
[2]*Department of Physics and Astronomy, and National Superconducting Cyclotron Laboratory, Michigan State University East Lansing, Michigan 48824-1321, USA*
(Received 13 August 2008; published 9 December 2008)

The new Hamiltonians USDA and USDB for the *sd* shell are used to calculate $M1$ and $E2$ moments and transition matrix elements, Gamow-Teller β-decay matrix elements, and spectroscopic factors for *sd*-shell nuclei from $A = 17$ to $A = 39$. The results are compared with those obtained with the older USD Hamiltonian and with experiment to explore the interaction sensitivity of these observables.

DOI: 10.1103/PhysRevC.78.064302 PACS number(s): 21.60.Cs, 21.10.Jx, 21.10.Ky, 23.20.−g

I. INTRODUCTION

Two new interactions, USDA and USDB [1], have recently been obtained from fits of 63 two-body matrix elements (TBME) and three single-particle energies to the experimental values for 608 energies (for the ground states and low-lying excited states) of the *sd*-shell nuclei from $A = 16$ to $A = 40$. These are used for configuration-interaction calculations involving the $0d_{5/2}$, $0d_{3/2}$, and $1s_{1/2}$ active orbitals for protons and neutrons. For USDA 30 linear combinations of one- and two-body matrix elements were varied, with the remaining 36 linear combinations fixed at values of a renormalized G matrix, with a resulting rms deviation between experimental and theoretical energies of 170 keV. For USDB, 56 linear combinations were varied with 10 fixed at the G-matrix values and with an improved rms deviation of 130 keV. The energy data set used for USDA and USDB was updated from the one used 25 years ago to obtain the USD interaction based on 47 linear combinations of parameters fitted to 447 energy data with an rms deviation of 150 keV [2]. The energy data have been improved and extended in particular with more recent data for the neutron-rich *sd*-shell nuclei. As a consequence the main change from USD to USDA/B in terms of energies of low-lying states involved the most neutron-rich nuclei, and in particular features related to the position of the neutron $d_{3/2}$ single-particle state around ^{24}O. Ground state energies and excitation energies for all *sd*-shell nuclei are shown in Ref. [3] and compared with experiment where available.

The values of the TBME for USD, USDA, and USDB are given in Table I of Ref. [1] and are compared graphically in Figs. 7 and 8 of Ref. [1]. Generally, the 28 diagaonal TBME (out of 63 total) of the form $\langle j_1, j_2, J, T|V|j_1, j_2, J, T\rangle$ are best determined by the fits to energy data. The TBME involving both $d_{5/2}$ and $d_{3/2}$ are relatively poorly determined by the energy data, because the 6–7 MeV single-particle energy splitting makes the contribution of these TBME to the energies of low-lying states relatively small.

In this work we explore the sensitivity of other observables to the differences in these three Hamiltonians. We consider $M1$ moments and γ-transition matrix elements (Sec. II), $E2$ moments and γ-transition matrix elements (Sec. III), Gamow-Teller (GT) β-transition matrix elements (Sec. IV), and spectroscopic factors (Sec. V). We compare the results of the interactions with each other as well as to experiment. In terms of individual two-body matrix elements the differences between the Hamiltonians are relatively large as observed in Fig. 7 of Ref. [1]. The observables we consider may be sensitive to parts of the Hamiltonian that are not well constrained by energy data.

The experimental data for $M1$ and $E2$ transition matrix elements [4] and for the Gamow-Teller matrix elements [5] are the same set used to test the original USD Hamiltonian. For $M1$ and $E2$ moments we use the recent compilation by Stone [6]. For ^{35}K a new value from Ref. [7] is used. The data for spectroscopic factors between ground states are taken from Tsang, Lee, and Lynch [8].

The electromagnetic and β-decay operators involve one-body operators that must be renormalized [4]. Thus for all of these we carry out least-square fits to data to determine the values of the parameters that enter in the operators. To determine the values and uncertainties of the parameters we assign uncertainties to each observable of the form

$$\sigma^2 = \sigma_{\rm exp}^2 + \sigma_{\rm th}^2, \tag{1}$$

where $\sigma_{\rm exp}$ is the experimental error for each datum and $\sigma_{\rm th}$ is a theoretical error for each type of observable. The theoretical error is chosen so that the χ^2 value is near unity.

II. MAGNETIC DIPOLE MOMENTS AND TRANSITIONS

The $M1$ operator is

$$(M1)^{\rm op} = \sqrt{\frac{3}{4\pi}}\Sigma_{i,\tau_z}\{g_{s\tau_z}\vec{s}_{i,\tau_z} + g_{\ell\tau_z}\vec{\ell}_{i,\tau_z} + g_{t\tau_z}\sqrt{8\pi}[Y^2(\hat{r}_{i,\tau_z})\otimes\vec{s}_{i,\tau_z}]^{(1)}\}\mu_N, \tag{2}$$

where the sum runs over the Z protons ($\tau_z = p$) and N neutrons ($\tau_z = n$). The last term in Eq. (2) is the so-called tensor $M1$ operator [9]. We consider results with the free-nucleon g factors $g_{\ell p} = 1$, $g_{sp} = 5.586$, $g_{tp} = 0$, $g(\ell n) = 0$, $g_{sn} = -3.826$, $g_{tn} = 0$, as well as with effective values for the these six terms obtained from a least-square fit to the $M1$ data (moments as well as transitions). The two

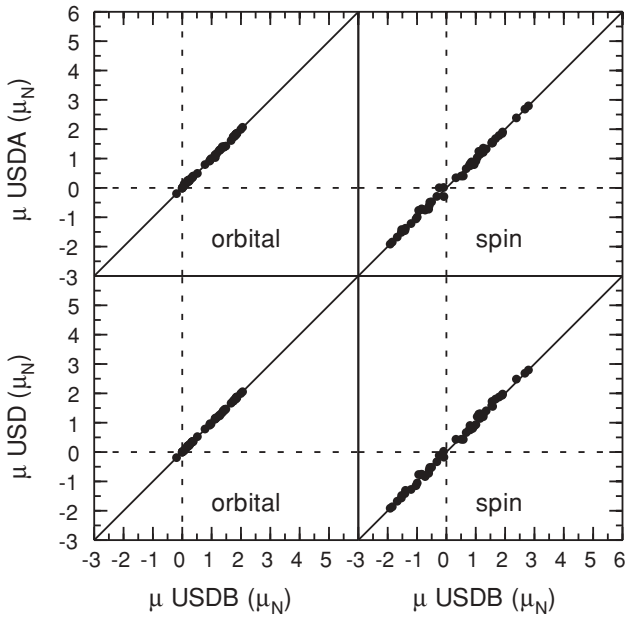

FIG. 1. Magnetic moments. Comparison of the orbital and spin contributions for the different Hamiltonians.

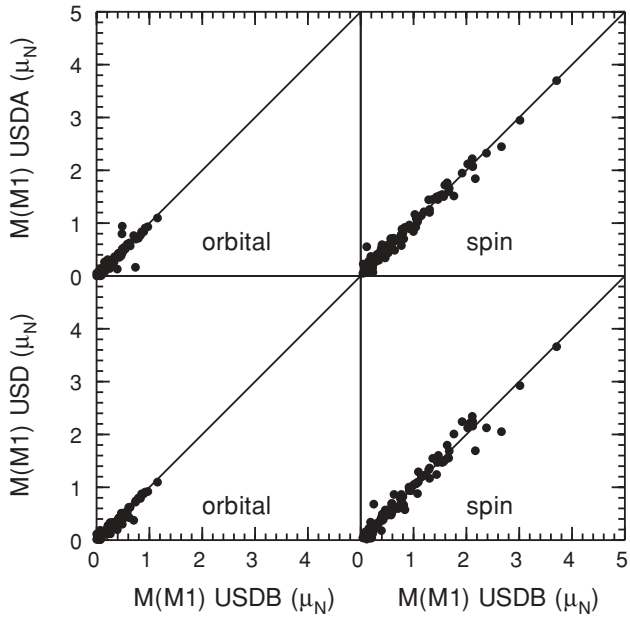

FIG. 2. $M1$ transition matrix elements. Comparison of the orbital and spin contributions for the different Hamiltonians.

observables are magnetic moments,

$$\mu = \sqrt{\frac{4\pi}{3}} \langle \Psi | (M1)^{\mathrm{op}} | \Psi \rangle_{M=J}, \tag{3}$$

and $M1$ transition matrix elements,

$$M(M1) = \langle \Psi_f \| (M1)^{\mathrm{op}} \| \Psi_i \rangle, \tag{4}$$

related to the $M1$ transition probabilities by $B(M1) = [M(M1)]^2/(2J_i + 1)$.

In the bottom panels of Figs. 1 and 2, the orbital and spin contributions from the USD and USDB calculations are compared (with free-nucleon g factors). In the top panels of Figs. 1 and 2 these contributions for USDA and USDB are compared. For moments (Fig. 1) one sees a very small Hamiltonian sensitivity. The Hamiltonian sensitivity is larger for $M1$ transitions (Fig. 2). The orbital contribution for USDB vs USDA shows three relatively large differences, and these are for the transitions $^{34}\mathrm{Cl} : 2_1^+, T = 1 \rightarrow 1_1^+, T = 0$, $^{34}\mathrm{Cl} : 1_2^+, T = 1 \rightarrow 0_1^+, T = 1$, and $^{34}\mathrm{Cl} : 1_2^+, T = 1 \rightarrow 0_1^+, T = 1$. Thus, a separate study of this (and other odd-odd) nucleus as a test of the Hamiltonians may be useful.

The differences for the spin contribution are much more scattered. The scatter is uniform as a function of mass number. The implication is that there are parts of the Hamiltonian (e.g., two-body matrix elements or linear combinations of two-body matrix elements) that are sensitive to these $M1$ data that are not well determined from the fits to energy data. Because the matrix element of the spin operator is large between the $d_{3/2}$ and $d_{5/2}$ orbitals, the spin contribution is sensitive to the mixing between $d_{3/2}$ and $d_{5/2}$ configurations in the low-lying states that is controlled by the off-diagaonal two-body matrix elements involving $d_{3/2}$ and $d_{5/2}$ orbitals. As noted in the Introduction, these are in fact the TBME that are the least well determined by the fits to energy data for low-lying states.

Comparison of theory with experiment is shown in Figs. 3 (for 48 magnetic moments) and 4 (for 111 $M1$ transitions).

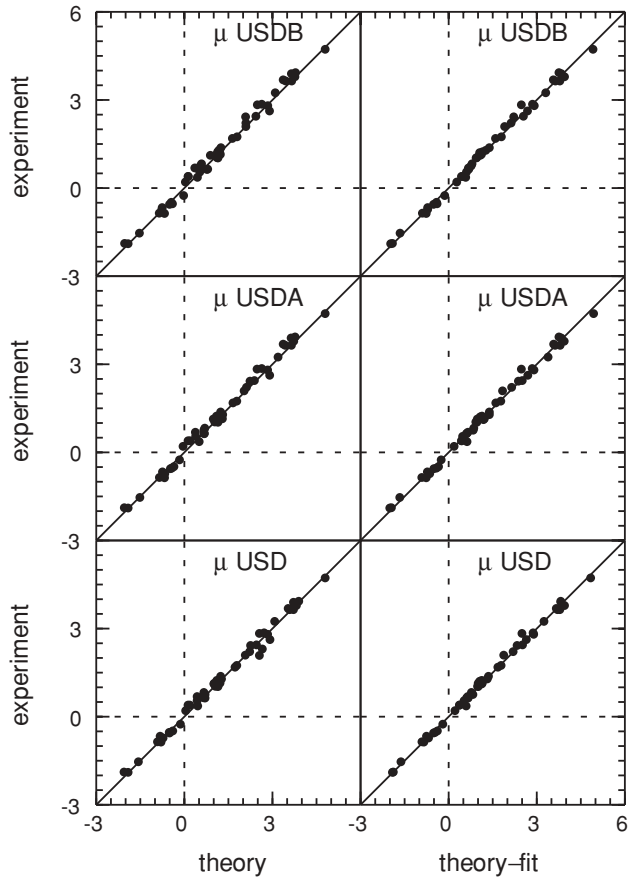

FIG. 3. Comparison of experiment and theory for magnetic moments.

TABLE I. Results for the rms deviation and effective g factors with the fits to $M1$ data with four ($N = 4$) and six parameters ($N = 6$) compared to the free-nucleon values ($N = 0$).

Hamiltonian (N)	$g_{\ell p}$	g_{sp}	g_{tp}	$g_{\ell n}$	g_{sn}	g_{tn}	rms μ	rms $M(M1)$
USD(0)	1	5.586	0	0	−3.826	0	0.125	0.264
USD(4)	1.114(23)	5.12(9)	0	−0.054(26)	−3.52(10)	0	0.104	0.241
USD(6)	1.137(24)	4.94(11)	0.34(9)	−0.079(28)	−3.38(13)	−0.22(11)	0.094	0.229
USDA(0)	1	5.586	0	0	−3.826	0	0.153	0.271
USDA(4)	1.155(23)	5.19(9)	0	−0.084(26)	−3.63(10)	0	0.124	0.236
USDA(6)	1.175(24)	5.00(11)	0.26(9)	−0.106(28)	−3.50(13)	−0.17(11)	0.118	0.223
USDB(0)	1	5.586	0	0	−3.826	0	0.165	0.252
USDB(4)	1.159(23)	5.15(9)	0	−0.09(26)	−3.55(10)	0	0.117	0.212
USDB(6)	1.174(24)	5.00(11)	0.24(9)	−0.11(28)	−3.44(13)	−0.16(11)	0.110	0.202

The sign for the magnetic moments of ^{19}O, ^{23}Mg, and ^{31}S, not determined by experiment, are taken from theory. Magnetic moments for neutron-rich Ne [10], Na [11], and Mg [12] *sd*-shell nuclei are not included. These are compared and discussed in comparison with theory at the end of this section. The agreement with experiment with the free-nucleon g factors is already fairly good. Use of the effective g factors leads to a visible improvement for both moments and transitions. Even though there are differences between the results for the different Hamiltonians, one cannot say any one of them is better.

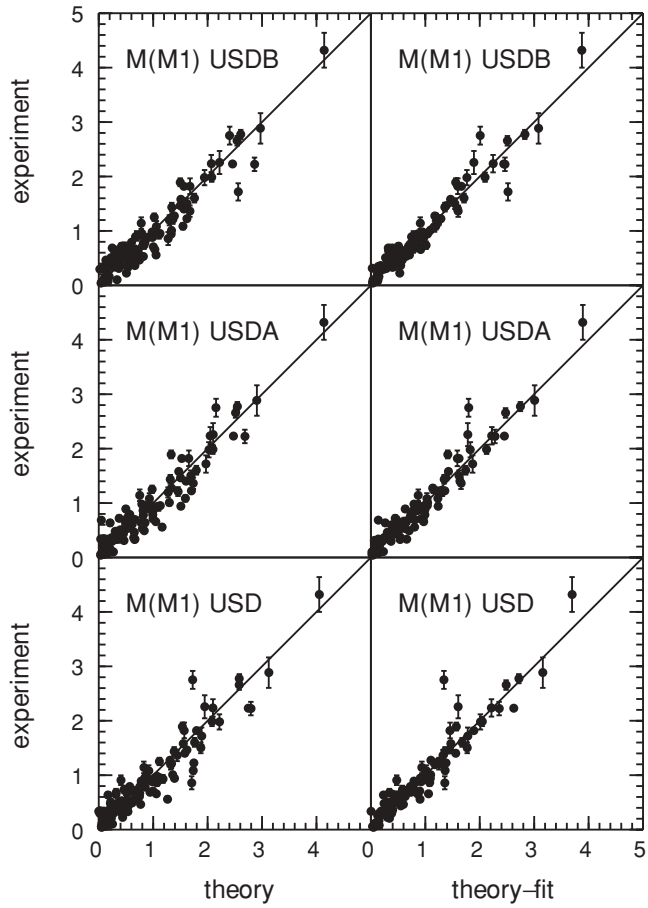

FIG. 4. Comparison of experiment and theory for $M1$ transition matrix elements.

The rms deviations and resulting values for the effective g factors are given in Table I (we used $\sigma_{\rm th} = 0.2$). The rms values for the deviation between experiment and theory for the $M1$ data are reduced from the free-nucleon values ($N = 0$) with the effective-operator fit, and all of the Hamiltonians give similar results for the rms deviations and effective g factors. There is a small but significant improvement in the rms deviations if the tensor-$M1$ terms are included in the fit ($N = 6$). There is a small dependence of the values of the effective g factors on the Hamiltonian, but they are within the uncertainties obtained for each fit. Thus, the previous work on the interpretation of the values of the effective $M1$ operator based upon the USD Hamiltonian [4] is still valid. Given (as discussed above) that there is some dependence of the calculated matrix elements on the Hamiltonian, we might expect a further reduction in the rms deviation (and reduction of the errors of the effective g factors) if the $M1$ data could be included in a fit of the Hamiltonian parameters to energy data.

We list in Table II magnetic moments of neutron-rich *sd*-shell nuclei, some of which have only recently been measured [10,12]. They are compared with theoretical predictions. Some of these, ^{30}Na, ^{31}Na, and ^{31}Mg, are well known to lie inside the island of inversion [13] (see the discussion on binding energies in Ref. [1]), and as expected the agreement between experiment and theory for these is not as good as the overall $\approx$0.10 μ_N rms deviation found for the six-parameter fits. The others are within the expected rms deviation, with somewhat better results obtained for USDA/B, as might be expected because these Hamiltonians included more energy data for nuclei outside of the island of inversion in this region of neutron-rich nuclei.

III. ELECTRIC QUADRUPOLE MOMENTS AND TRANSITIONS

The $E2$ operator is

$$(E2)^{\rm op} = \Sigma_{i,\tau_z} e_{\tau_z} r_{i,\tau_z}^2 Y^2(\hat{r}_{i,\tau_z}) e, \tag{5}$$

where the sum runs over the Z protons ($\tau_z = p$) and N neutrons ($\tau_z = n$). We consider results with the free-nucleon effective charges $e_p = 1$ and $e_n = 0$, as well as with effective values for

TABLE II. Experimental and calculated magnetic moments (in units of μ_N) for neutron-rich nuclei.

	USD(0)	USD(6)	USDA(0)	USDA(6)	USDB(0)	USDB(6)	Experiment	Ref.
^{23}Ne $5/2^+$	−1.128	−1.164	−1.013	−1.132	−1.050	−1.144	−1.077(4)	[10]
^{25}Ne $1/2^+$	−0.852	−0.821	−0.877	−0.871	−0.927	−0.898	−1.0062(5)	[10]
^{30}Na 2^+	2.554	2.693	2.444	2.648	2.418	2.596	2.083(10)	[11]
^{31}Na $3/2^+$	2.655	2.724	2.591	2.729	2.614	2.736	2.305(8)	[11]
^{27}Mg $1/2^+$	−0.420	−0.421	−0.353	−0.364	−0.412	−0.406	−0.4107(15)	[12]
^{29}Mg $3/2^+$	0.953	0.928	1.058	1.031	1.071	1.003	0.9780(6)	[12]
^{31}Mg $1/2^+$	−1.256	−1.051	−1.207	−1.036	−0.923	−0.730	−0.88355(15)	[12]

these two terms obtained from a least-square fit to the $E2$ data. The two observables are quadrupole moments,

$$Q = \sqrt{\frac{16\pi}{5}} \langle \Psi | (E2)^{\rm op} | \Psi \rangle_{M=J}, \tag{6}$$

and $E2$ transition matrix elements,

$$M_p = \langle \Psi_f \| (E2)^{\rm op} \| \Psi_i \rangle, \tag{7}$$

related to the $E2$ transition probabilities by $B(E2) = M_p^2/(2J_i + 1)$. We also write these in terms of the explicit proton and neutron components:

$$Q = e_p Q_p + e_n Q_n \tag{8}$$

and

$$M_p = e_p A_p + e_n A_n. \tag{9}$$

The radial matrix elements were calculated with harmonic-oscillator radial wave functions with oscillator lengths fitted to the rms charge radius of the stable isotopes [14].

The results for the three Hamiltonians are compared in Figs. 5 and 6 for both the proton components (Q_p and A_p) and the neutron components (Q_n and A_n) of the matrix elements. Except for a few points, the results are remarkably the same. The largest difference shows up in USDB vs USD for A_p and A_n, by the point near the coordinates $(0, 3)$ in the lower panels of Fig. 6. It corresponds to the ^{32}P $4_1^+ \rightarrow 2_1^+$ transition. The experimental matrix element for this transition is (in units of e fm^2) $M_p = 1.91(12)$ compared to the calculated results (with effective charges) of 5.30, 2.24, and 0.10 for USD, USDA, and USDB, respectively. So this singular point favors the USDA Hamiltonian. In the future we will make a complete comparison for odd-odd nuclei such as ^{30}P (and ^{34}Cl mentioned in Sec. II) as a more complete test of the Hamiltonians. For the other cases considered all of the Hamiltonians give essentially the same comparison to data which we show in the top panel of Figs. 5 (for 26 quadrupole moments) and 6 (for 144 $E2$ transitions) for experiment compared to the USDB results.

The least-square fit for the effective charges (with $\sigma_{\rm th} = 2.0\, e$ fm^2) gave essentially the same results for all three Hamiltonians: $e_p = 1.36(5)$ and $e_n = 0.45(5)$. As is well known the effective charge is essential for these $E2$ observables. There is a very large deviation with bare charges (left-hand side of the top panels in Figs. 5 and 6) giving systematically much too small theoretical values. The effective charges reproduce the data with rms deviations of 2.1 e fm^2 for $E2$ transitions and 1.9 e fm^2 for quadrupole moments. Because all three Hamiltonians give essentially the same result for this set of observables, all of the previous analysis obtained with the USD Hamiltonian about the dependence of the effective charges on the assumptions about the radial wave functions is still valid [4].

IV. GAMOW-TELLER TRANSITIONS

The Gamow-Teller (GT) β-decay operator is

$$({\rm GT})^{\rm op} = q_{\rm GT} \Sigma_i 2\, \vec{s}_i\, t_{\pm,i}, \tag{10}$$

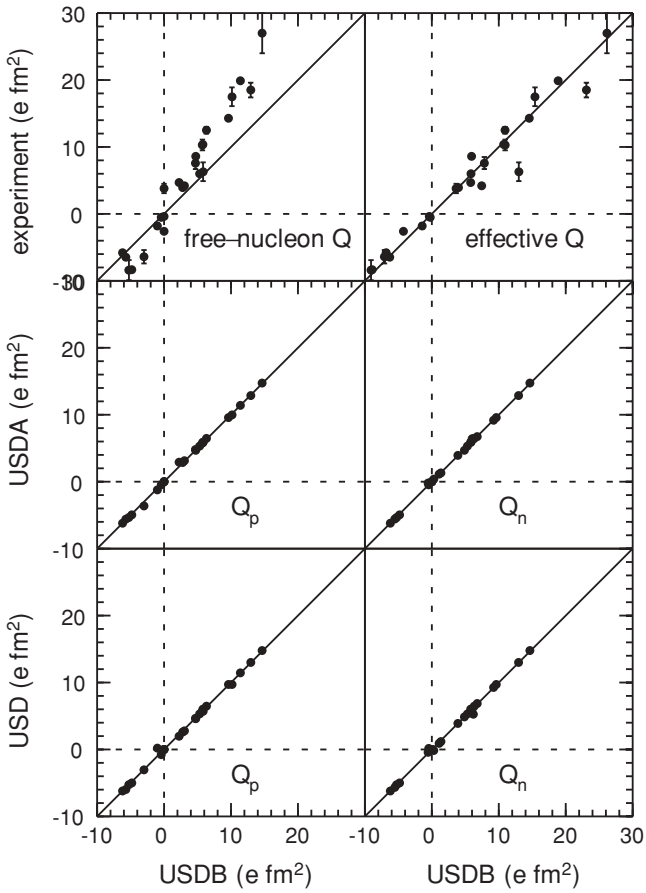

FIG. 5. Quadrupole moments. The lower panels show the comparison with the different Hamiltonians. The top panels show the comparison of experiment with the USDB calculations.

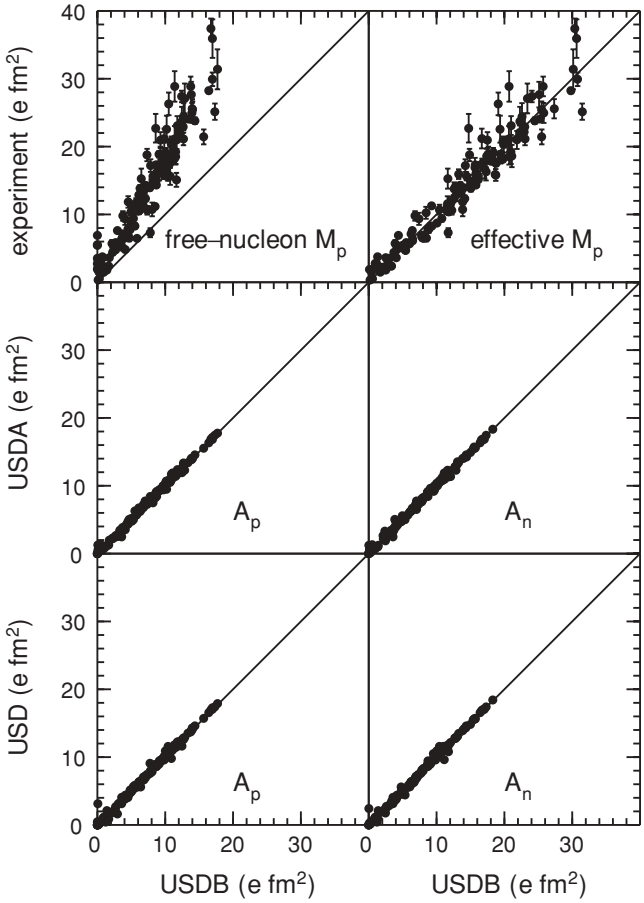

FIG. 6. $E2$ transition matrix elements. The lower panels show the comparison with the different Hamiltonians. The top panels show the comparison of experiment with the USDB calculations.

where the sum runs over the A nucleons and $t_\pm$ is the isospin raising-lowering operator. $q_{\rm GT}$ is an effective GT operator (parameter) normalized by its free-nucleon value of $q_{\rm GT} = 1$. The GT transition matrix elements are

$$M({\rm GT}) = \langle \Psi_f \| ({\rm GT})^{\rm op} \| \Psi_i \rangle, \qquad (11)$$

related to the GT transition probabilities by $B({\rm GT}) = [M({\rm GT})]^2/(2J_i + 1)$.

In Fig. 7 the M(GT) (with $q_{\rm GT} = 1$) for the matrix elements obtained with the three Hamiltonians are compared. In contrast to the results for $E2$, there is a scatter among the matrix elements. The scatter is uniform as a function of mass number. The scatter is similar to that observed for the $M1$ spin matrix element on the right-hand side of Fig. 2. As noted in Sec. II, this can be related to the TBME involving both the $d_{3/2}$ and $d_{5/2}$ orbitals, which are not well determined by the fits to the energy data for low-lying states. Thus, we may conclude that the inclusion of $M1$ and GT data in the determination of the Hamiltonian would help to increase the precision of the empirical interaction and its predictive power for $M1$ and GT observables.

The comparison of theory with experiment (232 data) is shown in Fig. 8. The results for the one-parameter fit ($\sigma_{\rm th} = 0.15$) to $q_{\rm GT}$ are given in Table III. The results for

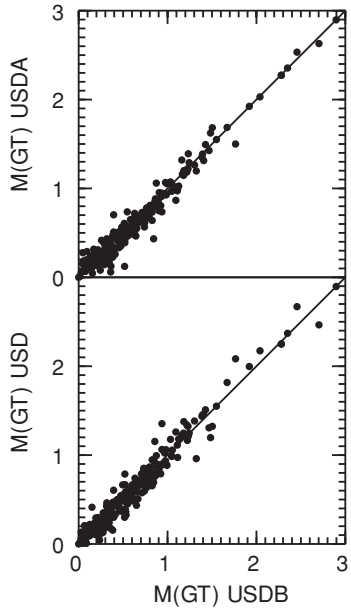

FIG. 7. Gamow-Teller β-decay matrix elements. Comparisons of the different Hamiltonians.

the values of $q_{\rm GT}$ do not depend on the Hamiltonian within the uncertainty. Thus, this quenching factor for GT transitions

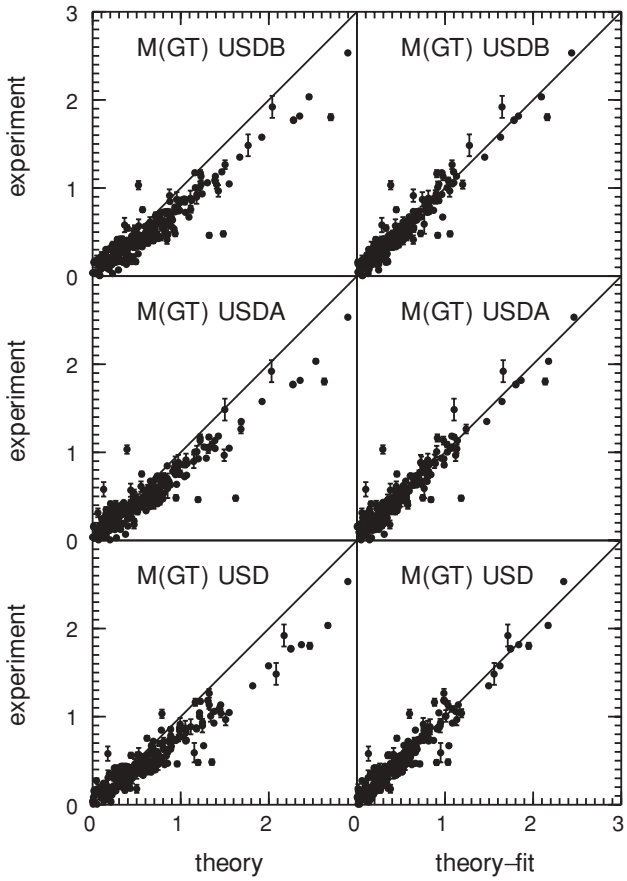

FIG. 8. Comparison of experiment and theory for Gamow-Teller decay matrix elements.

TABLE III. Results for the rms deviation for the free-nucleon ($N = 0$) and effective operators ($N = 1$) for Gamow-Teller matrix elements.

Hamiltonian (N)	q_{GT}	rms
USD(0)	1	0.219
USD(1)	0.776(13)	0.119
USDA(0)	1	0.213
USDA(1)	0.791(13)	0.136
USDB(0)	1	0.217
USDB(1)	0.764(13)	0.114

is very stable, and all of the conclusions discussed previously about its interpretation in terms of higher-order configuration mixing and Δ-particle admixtures [4] are still valid.

V. SPECTROSCOPIC FACTORS

The results for the basic set of ground state to ground state spectroscopic factors are shown in Fig. 9. The lower two panels compare theory, USDB vs USD and USDB vs USDA. The results are remarkably similar between the calculations. The data for spectroscopic factors between ground states are taken from Table I of from Tsang, Lee, and Lynch [8] (see also Ref. [15]). (The spectroscopic factor of 1.60 ± 0.23 given in Table I of Ref. [8] for ^{19}F(p,d)^{18}F appears to be that for the transfer to the 3^+ excited state of ^{18}F. We have replaced this with the value of 0.65 ± 0.10 from Ref. [16] obtained for the transfer to the 1^+ ground state.) Experiment is compared with values obtained with the USDB Hamiltonian in the top panel of Fig. 9. The agreement between experiment and theory is good.

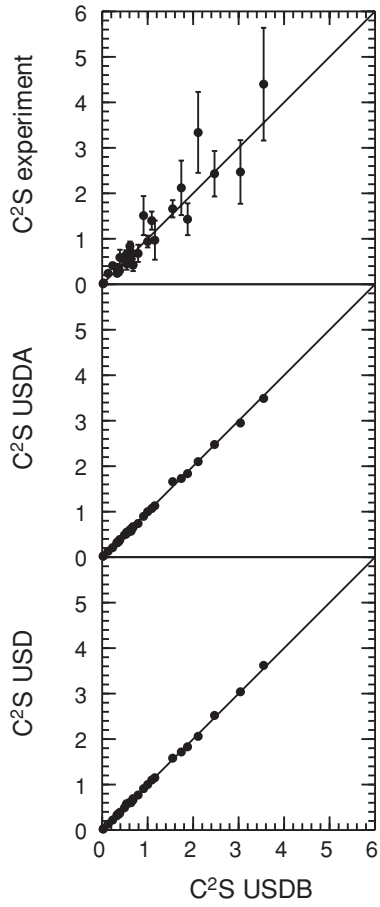

FIG. 9. A plot of experimental and theoretical single-nucleon spectroscopic factors for the three interactions USD, USDA, and USDB.

Spectroscopic factors extracted from (e,e′p) and high-energy nucleon knockout experiments for the sd-shell nuclei are systematically reduced by a factor of about 0.6 (for nuclei near stability) compared to theory [17]. The spectroscopic factors extracted from the analysis of Ref. [8] depend upon the optical potentials. Reasonable changes in the optical potential can lead to reduced values of the extracted spectroscopic factors that are closer to those obtained from (e,e′p) reactions [18,19].

VI. CONCLUSIONS

We have used three sd-shell Hamiltonians (USD, USDA, and USDB) to investigate observables that include $M1$ moments and $M1$ transition matrix elements, $E2$ moments and $E2$ transition matrix elements, Gamow-Teller β-decay matrix elements, and spectroscopic factors between ground states. For nuclei near stability all of these Hamiltonians give a similar description of the energies, whereas the recent USDA and USDB Hamiltonians are better for energies of neutron-rich sd-shell nuclei. Some linear combinations of two-body matrix elements are not well determined from the energy data and must be replaced by theoretical values based on renormalized G-matrix approximations. Thus, the predictions for these observables, which depend upon the Hamiltonian, provide a discriminating test and may lead to ways to further constrain the Hamiltonian and to improve the wave functions. Such improvements would decrease the uncertainties for the applications to nuclear astrophysics where the needed reaction rates depend entirely or in part on theoretical input for γ widths and spectroscopic factors [20].

We find that some of the observables are very insensitive to the Hamiltonians, these include the orbital contribution to the $M1$ matrix elements, the $E2$ matrix elements and the spectroscopic factors between ground states. There are just a few exceptions for the odd-odd nuclei, ^{30}P and ^{34}Cl, that warrant a more complete comparison for the gamma decay properties of these (and other odd-odd) nuclei that will be considered in the future.

The spin-matrix elements for $M1$ and GT are more sensitive to the Hamiltonians. There is a considerable scatter in these matrix elements calculated with the different Hamiltonians that is a little smaller than the scatter between theory and experiment. This may be related to the off-diagonal two-body matrix elements involving both $d_{3/2}$ and $d_{5/2}$ orbitals that are not well constrained by the fits to the energies of low-lying states. This suggests that a fit of the Hamiltonian two-body

matrix elements that includes energy and $M1$ and GT data would be able to improve the predictions for $M1$ and GT data and to provide a more completely constrained effective Hamiltonian for the sd shell.

The effective operators for the $M1$, $E2$, and GT observables are similar for all of the Hamiltonians. This means that all of the previous discussion [4] of the interpretation of these effective operators in terms of mesonic-exchange current, higher-order configuration mixing, and Δ-particle admixtures remains valid.

ACKNOWLEDGMENTS

This work is partly supported by NSF Grants PHY-0555366 and PHY-0758099 and by the National Research Foundation of South Africa under Grant 2073007.

[1] B. A. Brown and W. A. Richter, Phys. Rev. C **74**, 034315 (2006).
[2] B. H. Wildenthal, Prog. Part. Nucl. Phys. **11**, 5 (1984).
[3] B. A. Brown, http://www.nscl.msu.edu/∼brown/resources/resources.html.
[4] B. A. Brown and B. H. Wildenthal, Ann. Rev. Nucl. Part. Sci. **38**, 29 (1988).
[5] B. A. Brown and B. H. Wildenthal, At. Data Nucl. Data Tables **33**, 347 (1985).
[6] N. J. Stone, At. Data Nucl. Data Tables **90**, 75 (2005).
[7] T. J. Mertzimekis, P. F. Mantica, A. D. Davies, S. N. Liddick, and B. E. Tomlin, Phys. Rev. C **73**, 024318 (2006).
[8] M. B. Tsang, J. Lee, and W. G. Lynch, Phys. Rev. Lett. **95**, 222501 (2005).
[9] B. A. Brown and B. H. Wildenthal, Phys. Rev. C **28**, 2397 (1983).
[10] W. Geithner *et al.*, Phys. Rev. C **71**, 064319 (2005).
[11] G. Huber *et al.*, Phys. Rev. C **18**, 2342 (1978).
[12] M. Kowalska *et al.*, Phys. Rev. C **77**, 034307 (2008).
[13] E. K. Warburton, J. A. Becker, and B. A. Brown, Phys. Rev. C **41**, 1147 (1990).
[14] B. A. Brown, W. Chung, and B. H. Wildenthal, Phys. Rev. C **22**, 774 (1980).
[15] J. Lee, M. B. Tsang, and W. G. Lynch, Phys. Rev. C **75**, 064320 (2007).
[16] J. M. Delbrouck-Habaru and G. Robaye, Nucl. Phys. **A337**, 107 (1980).
[17] A. Gade *et al.*, Phys. Rev. C **77**, 044306 (2008).
[18] G. J. Kramer, H. P. Blok, and L. Lapikas, Nucl. Phys. **A679**, 267 (2001).
[19] J. Lee, J. A. Tostevin, B. A. Brown, F. Delaunay, W. G. Lynch, M. J. Saelim, and M. B. Tsang, Phys. Rev. C **73**, 044608 (2006).
[20] H. Schatz, C. A. Bertulani, B. A. Brown, R. R. C. Clement, A. A. Sakharuk, and B. M. Sherrill, Phys. Rev. C **72**, 065804 (2005).